International Journal of Electrical and Power Engineering 6 (1): 19-25, 2012
ISSN: 1990-7958

Selection of Effective Control Technique in Analysis of Pulsed Power Loads

D. Rajalakshmi and L. Jeniferamla
Department of Electrical and Electronics Engineering,
Kumaraguru College of Technology, Coimbatore, India

Abstract: This study considers the effect of Pulsed Power Loads (PPLs) on micro-grid power systems such as those on warships, pulsed weapons and recovery systems. A design metric to describe the disturbance of PPLs on power systems is shown. A control strategy utilizes the design metric to reduce the impact of PPL. This strategy is based on identifying the optimal charging profile. Using simulation, it is shown the proposed strategy is highly effective in reducing the adverse impact of pulsed-power loads by reducing the impulse response of capacitor current. This study outlines an approach to analyze the effects of such loads upon the electric power grid using the proposed technique Trapezoidal Based Control (TBC) and a charging profile is developed for the existing analysis technique Limit Based Control (LBC). Both the control techniques are compared to find the effective approach in reducing the impact of pulsed power loads.

Key words: Marine vehicles, military aircraft, power quality, energy storage, pulsed power systems, India

INTRODUCTION

Pulsed Power Loads (PPLs) are of significant interest in navy applications such as future warship development. It is often the case in such loads that the energy storage element is charged over a finite interval of time and then rapidly discharged (Crider and Sudhoff, 2010a). The charging of the energy storage device is an intermittent load which disturbs the power system. Examples of this class of system include high power radars, electromagnetic launch and recovery systems and pulsed weapons such as rail guns (Kulkarni and Santoso, 2009; van der Burgt *et al*., 1999). The power requirements of the charge cycle on such loads can extend into tens of megawatt range with a charge interval on the order of seconds to minutes (Smolleck *et al*., 1991). The discharge duration is normally much shorter and is often essentially instantaneous compared to the charge interval wherein energy is accumulated from the power system.

These pulses can cause significant disturbance to the rest of the power system (Kulkarni and Santoso, 2009; Domaschk *et al*., 2006). The goal of this research is to minimize the system impact of these Pulsed Power Loads (PPLs) by designing the capacitor current. This research begins with the development of a metric to describe the disturbance caused by a PPL (Crider and Sudhoff, 2010b). This metric is then solved to obtain an optimal power trajectory. A state feedback based approach to achieving this desired trajectory is then set forth. The PPL in this system uses capacitor energy storage and is designed to emulate a rail gun application. Through simulation studies, the performance of two types of control strategies such as Limit Based Control (LBC) and Trapezoidal Based Control (TBC) is compared to obtain an effective approach. It is shown that the performance of the proposed control (TBC) is significantly superior to the existing control (LBC) in terms of reducing the impulse response of capacitor current. One method to reduce the impact of pulsed loads is through the introduction of supplementary energy storage devices such as flywheels (Kulkarni and Santoso, 2009; Domaschk *et al*., 2006).

While effective such an approach clearly adds mass and expense to the system. Another method to reduce the disruption caused by PPLs is through load coordination. In such an approach, the base load is shed in order to accommodate the pulsed load so that, the total system load remains constant. Such an approach is considered by Domaschk *et al*. (2006), Cassimere *et al*. (2005) and Sudhoff *et al*. (2003). As an alternative to LBC, auxiliary energy storage and coordination strategies a Trapezoidal-Based Control (TBC) was set forth. This control was based on using a trapezoidal load profile. The parameters governing the shape of the trapezoid were selected so as to minimize the disruption caused by the pulsed load. However, this research assumed a priori that the trapezoidal power profile was the optimal shape. Here using simulation, it is proved that the proposed scheme is effective in reducing the impact of PPL by eliminating the impulse response. And a charging profile is developed for the existing control to identify the optimal trajectory.

Corresponding Author: D. Rajalakshmi, Department of Electrical and Electronics Engineering, Kumaraguru Colege of Technology, Coimbatore, India

MATERIALS AND METHODS

Circuit description: The circuit topology of the PPL is shown in Fig. 1. The circuit includes an input filter and a buck converter. The input filter is designed to reduce the high frequency current ripple associated with the buck converter from entering the power distribution system. The buck converter regulates the current i_1, so as to charge the energy storage capacitor C_{es} according to the desired profile. The pulsed load is that part of the PPL which discharges the capacitor. The storage capacitor used here plays an important role in PPL. The aim is to charge and discharge the capacitor as soon as possible subjected to current and power limits. This study is entirely concerned with the generation of capacitor current and thereby reducing the impulse response obtained during charging and discharging of capacitor. In the circuit, the energy storage capacitor is emulated so that the energy storage does not need to be physically achieved and to make it easier to achieve the appearance of a rapid discharge.

Design metric and normalizations: The 1st step in minimizing the system impact of the PPL is to define a metric to describe the disturbance caused by the PPL. A natural choice for such a metric would be related to the bus voltage during and after the PPL charge cycle. However, the problem with such an approach is that the evaluation of the metric becomes not only a function of the PPL but also of the system and thereby every component and control parameter therein. Thus in this research, an alternate metric is proposed, one which only involves the PPL. The disturbance of a PPL on a system is related to its time power profile. This profile is denoted as P_p (t) and is referred to as the power trajectory herein.

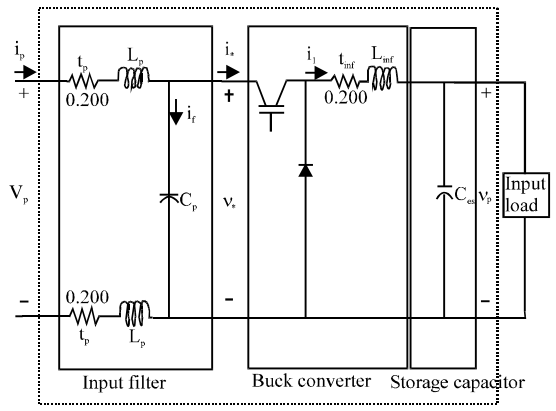

Fig. 1: Circuit diagram

The power trajectory must satisfy several constraints. First, the power trajectory must be such that the desired energy is obtained. Thus:

$$\int_0^{T_p} P_p(t)dt=\Delta E_p^* \quad (1)$$

Where:

ΔE_{p^*} = Incremental additional energy to be stored in the energy storage element during the charge cycle

T_p = Period of the charge cycle. Note that prior to the charge cycle, the amount of energy stored is not necessarily zero

E_{po} = This initial energy storage

Second, it is desirable that the power trajectory is a continuous function of time. Thus, it is required that:

$$P_p(t) \in C_o \quad (2)$$

Where, C_o is set of continuous functions. This facilitates implementation in the presence of parasitics and also limits the bandwidth of the PPL disturbance on the system. By definition, a pulsed load is an intermittent transient load. Requirement (Eq. 2) is thus coupled with the requirement that:

$$P_p(0) = P_p(T_p) = 0 \quad (3)$$

Finally, it is desired that the system disturbance caused by the trajectory is minimized. In order to quantify this last point, observe that if the PPL were not pulsed, i.e., were a constant then there would be no disturbance at all. Hence, one philosophy for a disturbance metric is to define the metric in terms of the time rate of change of the power trajectory. To this end, the disturbance metric is proposed as:

$$d_p = \sqrt{\frac{1}{T_p}\int_0^{T_p}\left(\frac{dP_p(t)}{dt}\right)^2 dt} \quad (4)$$

In Eq. 4, dP_p/dt is the time rate of change of power into the PPL. Before proceeding to explore the solution to this problem, it is convenient to normalize quantities of interest so that the results are readily scaled. To this end, the base energy will:

$$E_p^{\wedge} = \frac{\left(E_p - E_{po}\right)}{\Delta E_p^*} \quad (5)$$

Next, time is normalized to the charge cycle period T_p. Thus, normalized time is defined:

$$t^{\wedge} = \frac{t}{T_p} \tag{6}$$

Finally, the base power is defined as:

$$P_{p,b} = \frac{E_p^{**}}{T_p} \tag{7}$$

Where, upon normalized power may be expressed:

$$P_p^{\wedge}(t) = \frac{P_p(t)}{P_{p,b}} \tag{8}$$

In terms of normalized quantities, Eq. 1-4 become, respectively:

$$\int_0^1 P_p^{\wedge}\left(t^{\wedge}\right)dt^{\wedge} = 1 \tag{9}$$

$$P_p^{\wedge}\left(t^{\wedge}\right) \in C_o \tag{10}$$

$$P_p^{\wedge}(0) = P_p^{\wedge}(1) = 0 \tag{11}$$

$$dp^{\wedge} = \frac{d_p T_p}{P_{p,b}} = \sqrt{\int_0^1 \left(\frac{dP_p^{\wedge}(t)}{dt^{\wedge}}\right)^2 dt^{\wedge}} \tag{12}$$

The metric function and constraints can be solved to find the optimal power trajectory. The next section of this study will show this by applying the metric to a desired power profile.

Optimal trapezoidal trajectory: In this study, the metric will be used to find the optimal power trajectory subject to a trapezoidal power profile. This case is of interest because of its straightforward implementation. The trapezoidal power trajectory is shown in Fig. 2 where $t_r^{\wedge}$ is the normalized rise time $t_f^{\wedge}$ is the normalized fall time and $P_{pk}^{\wedge}$ is the normalized peak power.

Finding the optimal trajectory involves finding the parameters of the trapezoid which minimize the performance metric. As a prologue to this optimization, it is convenient to define the objective:

$$g_p^{\wedge} = d_p^{\wedge 2} \tag{13}$$

Therefore, Eq. 12 becomes:

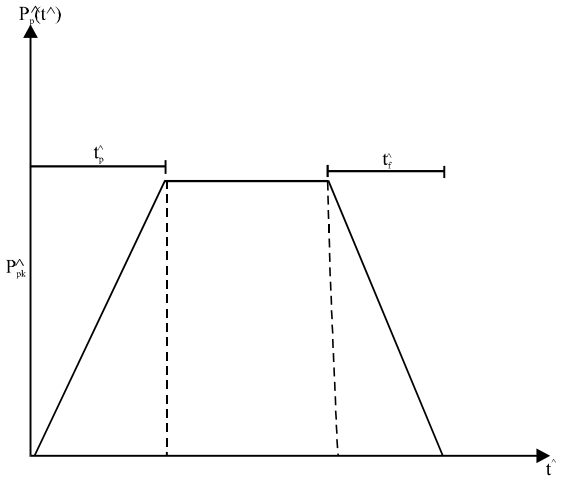

Fig. 2: Trapezoidal power trajectory

$$g_p^{\wedge} = \int_0^1 \left(\frac{dP_p^{\wedge}\left(t^{\wedge}\right)}{dt}\right)^2 dt \tag{14}$$

Minimization of $g_p^{\wedge}$ is exactly equivalent to minimization of $d_p^{\wedge}$ but results in a simpler development. Mathematically, the trapezoidal trajectory may be expressed:

$$P_p^{\wedge}\left(t^{\wedge}\right) = \begin{Bmatrix} \frac{P_{pk}^{\wedge}}{t^{\wedge}} t^{\wedge}\left(t^{\wedge} \le t_r^{\wedge}\right) \\ P_{pk}^{\wedge}(t_r^{\wedge} < t^{\wedge} \le 1 - t_f^{\wedge}) \\ \frac{-P_{pk}^{\wedge}}{t_f^{\wedge}} t^{\wedge} + \frac{P_{pk}^{\wedge}}{t_f^{\wedge}} (1 - t_f^{\wedge} < t^{\wedge} \le 1 \end{Bmatrix} \tag{15}$$

Substitution of Eq. 15 into Eq. 9 yields the constraint:

$$P_{pk}^{\wedge}\left(1 - \frac{t_r^{\wedge}}{2} - \frac{t_f^{\wedge}}{2}\right) = 1 \tag{16}$$

The time derivative of the trapezoidal profile is given by:

$$\frac{dP_p^{\wedge}}{dt^{\wedge}} = \begin{Bmatrix} \frac{P_{pk}^{\wedge}}{t_r^{\wedge}} (t^{\wedge} \le t_r^{\wedge}) \\ 0(t_r^{\wedge} < t^{\wedge} \le 1 - \le t_f^{\wedge}) \\ \frac{-P_{pk}^{\wedge}}{t_f^{\wedge}} (1 - t_f^{\wedge} < t^{\wedge} \le 1) \end{Bmatrix} \tag{17}$$

Substitution of Eq. 17 into Eq. 14 yields:

$$g_p^{\wedge} = P_{pk}^{\wedge 2}\left(\frac{1}{t_r^{\wedge}} - \frac{1}{t_f^{\wedge}}\right) \tag{18}$$

Combining the constraint Eq. 16 and 18 manipulating yields:

$$g_p^{\wedge} = \frac{1}{\left(1-\frac{t_S^{\wedge}}{2}\right)^2}\frac{4t_S^{\wedge}}{\left(t_S^{\wedge 2} - t_{\Delta}^{\wedge 2}\right)} \quad (19)$$

where:

$$t_S^{\wedge} = t_r^{\wedge} + t_f^{\wedge} \quad (20)$$

Equation 15 an can be viewed as a parametric relationship between $P_p^{\wedge}$ and $E_p^{\wedge}$ Eliminating from the parametric relationship yields:

$$P_p^{\wedge} = f_p\left(E_p^{\wedge}\right) = \begin{cases} \frac{3}{2}\sqrt{4E_p^{\wedge}}\,K\,K\,K\,K\ (E_p^{\wedge} \le \frac{1}{4}) \\ \frac{3}{2}K\,K\,K\,K\,K\ (\frac{1}{4} < E_p^{\wedge} \le \frac{3}{4}) \\ \frac{3}{2}\sqrt{-4(E_p^{\wedge}-1)}K\ \frac{3}{4} < E_p^{\wedge} \le 1 \end{cases} \quad (21)$$

Suggested values for $E_{LT}^{\wedge}$ and $E_{HT}^{\wedge}$ range from 0.001-0.05 and 0.95-0.999, respectively. At this point, a new control method derived from the metric to minimize system impact of the PPL has been presented.

RESULTS AND DISCUSSION

Control description: The control description of pulsed power loads can be described by charge discharge control and capacitor current command synthesizer. The charge discharge layer formulates charge and discharge commands and the current synthesizer utilize the desired charge profile and generate the capacitor current accordingly.

Charge discharge control: The charge/discharge control is presented by Steurer *et al.* (2007) shows a modified control used herein. The difference between the control by Steurer *et al.* (2007) and this control is the addition of the one-shot or control variable. The inputs to the control are a command to enable the charging of the capacitor, a command to discharge, the filtered voltage across the energy storage capacitor, the desired capacitor voltage for firing and the current measured voltage of the energy storage capacitor. The outputs of this control are the actual charging status, (high to charge) and the actual discharge status, (high to discharge). Provided that a discharge sequence is not underway and that the capacitor voltage is below the voltage sufficient for firing, setting high will cause the charge status to go high, whereupon the capacitor will be charged. The oneshot

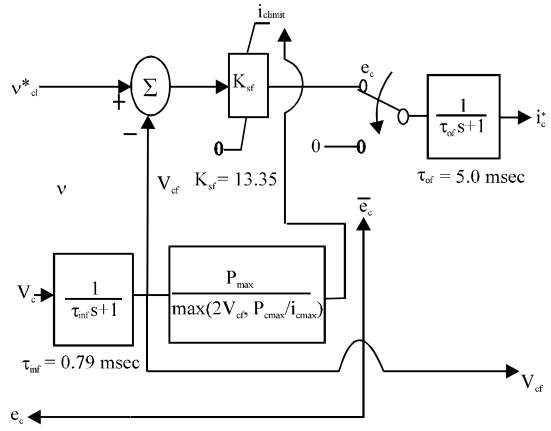

Fig. 3: LBC current command synthesizer

flag is high if a single shot is desired and low if it is desired to repeatedly go through the firing sequence as rapidly as possible. If is reset after a charge period, the PPL will repeat the charge and discharge sequence. If the energy storage capacitor voltage is above the threshold when the oneshot flag is enabled and if is high, a discharge sequence is enabled. During the discharge sequence, the net effect of the control is that the charge status will be disabled for a period of time defined by and the discharge status will be enabled for the last seconds of this cycle. This provides a short period of time when both the charge and discharge cycles are disabled.

Capacitor current synthesizer: This layer of the control formulates the capacitor current command. The proposed control scheme trapezoidal based control is set forth. Therefore, the two control schemes will be considered and compared. The first control scheme charges the capacitor as rapidly as possible subject to current and power limits without including a storage time, the waveform is parabolic. The second control scheme generates the capacitor current which makes use of storage time. The shape of the waveform is trapezoidal. This scheme was suggested by Bash *et al.* (2009). The second control scheme is the one proposed herein.

Current and power Limit Based Current Command synthesizer (LBC): The current and power limit based current command synthesizer control is shown in Fig. 3. The basic philosophy of the control is to charge the capacitor as rapidly as possible subject to a peak capacitor current limit i_{cmax} and a peak power limit P_{cmax} Inputs to this control are the target final capacitor voltage, v_{cl}^* the measured capacitor voltage $v_c^{\wedge}$ and the charge status, e_c. As can be seen, the measured capacitor voltage is first filtered by a low pass filter with time constant t_{inf} and then subtracted from the command.

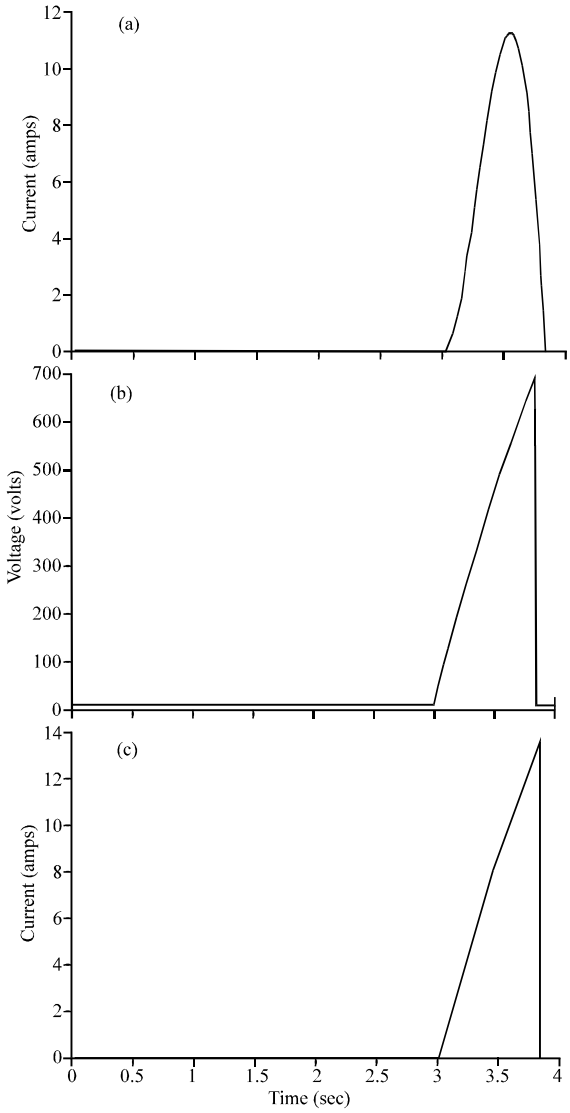

Fig. 4: a) Capacitor current, i_c; b) load voltage, V_L; c) GTO current

The voltage error is then multiplied by a proportional gain K_{sf} and limited to a dynamic limit i_{climit}. Note that K_{sf} is selected to be large enough that the limit is almost always in effect until the point where V_{cf} becomes very close to v_{c1}* after this point the capacitor voltage approaches the target voltage asymptotically. For this reason, the target voltage v_{c1}* is set slightly higher than the minimum voltage to fire, v_{c2}*.

The output of above control is capacitor current, i_c which is derived and then plotted using simulation. The simulation results are shown in Fig. 4a-c, the parameters such as capacitor current, i_c, load voltage, V_L, input current, i_c are plotted. The simulation parameters for limit based control are shown in Table 1.

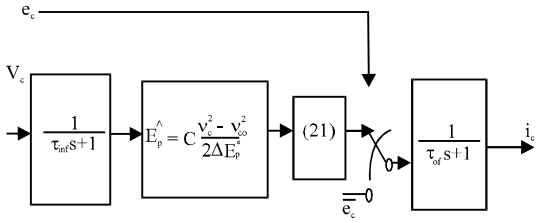

Fig. 5: TBC current command synthesizer

Table 1: LBC simulation parameters

v_{c1}*	410 V	Target capacitor firing voltage
v_{c2}*	405 V	Minimum capacitor firing voltage
P_{cmax}	13.52 kW	Capacitor power limit
i_{cmax}	40.52 A	Capacitor current limit

Table 2: TBC simulation parameters

Parameters	Values	Description
T_{inf}	0.79 msec	Time constant input filter
T_{of}	5.0 msec	Time constant of output filter
K_{of}	13.35	Current forward gain

TBC transient study results (simulation)

Trapezoidal capacitor current command synthesizer (TBC): The trapezoidal capacitor current command synthesizer control or Trapezoid Based Control (TBC) is based on Eq. 21. Note that this synthesizer results is a trapezoidal power profile; the capacitor current is a trapezoidal waveform. Like the LBC current command synthesizer, the output of this control is i_c*. The control is shown in Fig. 5. The inputs to the control are the measured capacitor voltage v_c and the charge status, e_c. As can be seen, the measured capacitor voltage is filtered and fed into the normalized energy block (Eq. 5). This normalized energy is then fed into the current command synthesis block determines the preliminary current command. The output of the synthesizer is the capacitor current command which is the output of the command synthesis block switched by the status of e_c. The control parameters for the TBC are shown in Table 2. The control parameters are used in estimation of capacitor current, i_c, mathematically.

It is proved that the mathematical calculation is almost equal to the simulation result. It is found that the mathematically calculated value of i_c is 11.2 A and from simulation results it can be seen that the capacitor current value is 11 A as shown in Fig. 6. In this study, simulation results for the two control methods are presented. A comparison of the disturbance to the system caused by both controls is presented. First, the simulation result for limit based control with the capacitor current of 11 A is generated as per the metric described above and the corresponding load voltage of 700 V is obtained.

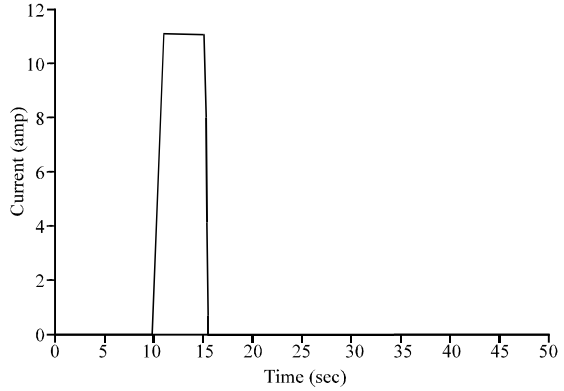

Fig. 6: Capacitor current

Second, a simulation result for the trapezoidal control with a capacitor current of 11A is obtained. These results illustrate that the effect of pulsed power loads is reduced using trapezoidal based control. The impulse response of LBC is eliminated using TBC.

LBC Study: In this study, the system is initially in steady-state. At t = 3 sec, a charging cycle is initiated. The goal is to charge the capacitor from 0-162 kJ in 3.8 sec. Figure 6a, b shows the results for the LBC. Variables depicted include the PPL capacitor current, i_c, the PPL load voltage, V_L, the dc current into the PPL and the current in the GTO. These variables are all defined in Fig. 4a-c. As can be seen, the capacitor voltage ramps up nearly linearly in time although, there is a slight inflection at 3.5 sec which corresponds to the control switching from the capacitor current limit to the power limit. The bus voltage is seen to gradually droop during the course of the charge cycle, however at the end of the charge cycle, the bus voltage rises sharply and a pronounced peak occurs. The input current can be seen to rise nearly linearly until the control enters constant power mode at which point the input current becomes constant. The peak value of input current is 14 A the current goes down as the power limit takes effect. The results of LBC are purely based on capacitor current derivation. It can be seen that the waveform is parabolic. The storage time is not included, the capacitor is charged in 0.5 sec and then rapidly discharged in 0.5 sec and the load responds when the capacitor charges and discharges. Thus, an optimal trajectory is formulated for the existing control.

TBC Study: Figure 6 shows the performance of the TBC control. In this case, the capacitor current i_c is a trapezoidal waveform which eliminates the impulse response of the load. The aim of this control is to charge and discharge the capacitor as rapidly as possible with a short storage time. Thus, the capacitor is charged in 0.5 sec and discharged in 0.5 sec with a storage time of 4 sec depending upon the application. The sudden dip in load voltage and current is avoided in this case. Due to the above result the sudden drop of voltage and current does not occur. The storage time is introduced in this strategy so that the load is not disturbed during the discharge of current. Thus this method is proved to be superior in eliminating the impulse response and thus it reduces the impact of pulsed power loads. It can be seen that, the capacitor current rises upto 11A as in LBC. The most significant difference between the two strategies in terms of waveform are the capacitor current, i_c. This result shows an advantage of the TBC over the LBC in its ability to function in large scenarios.

CONCLUSION

A metric for describing the impact of PPLs on micro-grid power systems has been presented. This metric has been solved for an optimal power trajectory subject to a trapezoidal power profile in proposed scheme. The existing scheme is solved for a parabolic charging profile. The trapezoidal trajectory has been utilized in an application setting to validate its improvement to the power system. Thus, the charging and discharging of an energy storage element will not disturb the power system. The results show that the developed power trajectory of trapezoidal control reduces the impact on the pulsed power loads by eliminating the impulse response as compared to the limit based control.

REFERENCES

Bash, M., R.R. Chan, J. Crider, C. Harianto and J. Lian *et al*., 2009. Medium voltage DC testbed for ship power system research. Proceedings of the IEEE Electric Ship Technologies Symposium, April 20-22, 2009, Baltimore, MD., pp: 560-567.

Cassimere, B., C.R. Valdez, S. Sudhoff, S. Pekarek, B. Kuhn, D. Delisle and E. Zivi, 2005. System impact of pulsed power loads on a laboratory scale Integrated Fight Through Power (IFTP) system. Proceedings of the IEEE Electric Ship Technologies Symposium, July 25-27, 2005, Philadelphia, pp: 176-183.

Crider, J. and S.D. Sudhoff, 2010a. Reducing power system impact of pulsed power loads. Proceedings of the Electric Machinery Technology Symposium, May 19-20, 2010, Philadelphia.

Crider, J. and S.D. Sudhoff, 2010b. Reducing impact of pulse power loads on microgrid power systems. IEEE Trans. Smart Grid, 1: 270-277.

Domaschk, L.N., A. Ouroua, R.E. Hebner, O.E. Bowlin and W.B. Colson, 2006. Coordination of large pulsed loads on future electric ships. Electromagn. Launch Technol. Symp., 43: 450-455.

Kulkarni, S. and S. Santoso, 2009. Impact of pulse loads on electric ship power system: With and without flywheel energy storage systems. IEEE Electric Ship Technol. Symp.10.1109/ESTS.2009. 4906568.

Smolleck, H.A., S.J. Ranade, N.R. Prasad and R.O. Velasco, 1991. Effects of pulsed-power loads upon an electric power grid. Trans. Power Del., 6: 1629-1640.

Steurer, M., M. Andrus, J. Langston, L. Qi, S. Suryanarayanan, S. Woodruff and P.F. Ribeiro, 2007. Investigating the impact of pulsed power charging demands on shipboard power quality. Proceedings of the IEEE Electric Ship Technologies Symposium, May 21-23, 2007, Arlington, VA., pp: 315-321.

Sudhoff, S.D., B.T. Kuhn, E. Zivi, D.E. Delisle and D. Clayton, 2003. Impact of pulsed power loads on naval power and propulsion systems. Proceedings of the 13th International Ship Control System Symposium, April 7-9, 2003, Orlando, FL.

Van der Burgt, J.J.A., P. van Gelder and E. van Dijk, 1999. Pulsed power requirements for future naval ships. Digest Tech. Pap., 2: 1357-1360.